

# Monitoring of Land Use Dynamics in the Autonomous District of Abidjan Between 2002 and 2022 using the Google Earth Engine Platform

**Kinakpefan Michel Traore**

Department of Geography, Jean Lorougnon Guédé University, Daloa, Côte d'Ivoire,

DOI: <https://doi.org/10.52403/ijrr.20230532>

## ABSTRACT

In the countries of the South, capital cities such as the Autonomous District of Abidjan polarize both economic activity and demographic growth to such an extent that they are subject to rapid land artificialisation. This artificialization, in conjunction with poorly controlled urbanization, contributes to the thinning of vegetated areas. The objective of this work is to determine the changes in land use and land cover that have occurred in the Autonomous District of Abidjan over the last two decades, 2002 and 2022. The method uses the Random Forest classification algorithm in the Google Earth Engine platform from Landsat composite images. With an overall accuracy of 98.03% in 2002 and 98.7% in 2022 and kappa coefficients of 0.9 in 2002 and 2022, the cartographic and statistical results show important dynamics in land use in the Autonomous District of Abidjan during this period. These dynamics are characterized by a regression of vegetated and hydrographic areas that have lost 61% of their surface to the benefit of the habitat that has increased by 171% from 22.4 thousand hectares to 55.4 thousand hectares.

**Keywords:** Autonomous District of Abidjan, random forest, google earth engine, urban dynamics, land use and land cover

## INTRODUCTION

In African countries with high population growth, one of the main challenges is the rapid urbanization of the population. Indeed, in the global population growth outlook, the urban population is expected to increase by 2.5 billion urban dwellers between 2018 -

2050 and nearly 90% of this increase will be concentrated in Asia and Africa (UNITED NATIONS, 2019). In Côte d'Ivoire, despite the recent surge of small and medium-sized cities, the country's strong urban growth remains strongly the preserve of the Autonomous District of Abidjan (ADA) (SDUGA, 2015). The population of this capital territory of Côte d'Ivoire increased from 17 thousand in 1934 to 6.3 million in 2021 (INS, 1992; INS, 2001; INS, 2021). In less than a century, this population has increased by more than 37,000% for an average annual growth rate of about 6.9%. Thus, more than one out of five inhabitants of Côte d'Ivoire (21.5%) reside in the ADA. This population corresponds to more than two out of five urban dwellers in the country (41%).

This demographic primacy in conjunction with a polarization of more than 80% of economic activity (WORLD BANK GROUP, 2019), inexorably implies a significant artificialization of land and the multiplication of built-up areas. Rapid urban and peri-urban growth puts increased pressure on vegetation cover (M. DALLIMER et al, 2011; D. N. RICHARDS and R. N. BELCHER, 2020) and exacerbates imbalances in fragile ecosystems such as wetlands (D. SYLLA and L. M-C AKADJE-KONAN, 2022). This thinning of urban vegetation appears to be a threat to the sustainable development of cities. Indeed, as D. N. RICHARDS and R. N. BELCHER (2020), urban vegetation

provides many ecosystem services that make cities more livable for city dwellers. These environmental services include regulating urban microclimates, reducing flood risk, and conserving biodiversity (T. ELMQVIST et al, 2015; J. BENINDE et al, 2015; D. N. RICHARDS and R. N. BELCHER, 2020). These vegetated spaces ineluctably participate in healthier, more user-friendly, and recreational cities that contribute to improved human health (K. TZOULAS et al 2007; H. LAI et al, 2019; D. N. RICHARDS and R. N. BELCHER, 2020).

All in all, without planning, many recent studies have shown that ongoing changes in land use and land cover due to anthropogenic actions are increasingly negatively impacting various aspects of the Earth's surface, such as terrestrial ecosystems, water balance, biodiversity, temperature enhancement, rainfall pattern variability, and extreme event frequencies (F. DUBERTRET et al, 2022, T. N. PHAN et al, 2020, L. KOSCHKE et al, 2012; S. NIQUISSE et al, 2017; N. A. WAHAP and H. Z. SHARFRI, 2020; S. S. TRAORE, 2022; A. A OSSENI, 2023; C. T FAYE et al, 2023). As the DAA will have more than 10 million inhabitants in 2050, monitoring changes in land use and land cover patterns with their implications on the natural environments now appears to be an urgent matter and a challenge for the sustainability of this capital territory of Côte d'Ivoire.

The study is part of this perspective of monitoring the dynamics of past and present land cover allocations. It assesses and maps changes in land use and land cover in the ADA between 2002 and 2022 using remote sensing technology. This technology has become more democratized and established as a practical, rapid, and efficient tool for mapping land cover and monitoring its change over time in recent decades (D. P. ROY et al, 2014; M. A. WULDER et al 2016; T. N. PHAN et al, 2020, S. ZHANG et al 2021; J. CUI et al, 2022).

However, as rightly pointed out by F. DUBERTRET et al (2022), performing

analysis on large spatial and temporal scales requires overcoming many technical challenges, such as rectifying differences between multiple sensors over different time periods, or taking into account heterogeneous data quality and availability due to various factors, including cloud cover. It would be tedious to perform all these surface information collection, storage, processing, and retrieval operations on a large scale using traditional methods (T. N. PHAAN et al, 2020, J. CUI et al, 2022).

Also, Google Earth Engine (GEE) which is an open-source JavaScript application programming interface presents itself as a new approach capable of overcoming these pitfalls and improving the results of image classification and land use/land cover modeling (F. CASU et al, 2017; N. GORELICK et al, 2017; M. A. WULDER et al, 2018; S. XIE et al, 2019; J. XU et al, 2021; F. DUBERTRET et al, 2022). This cloud-based geospatial analysis platform solves the most important problems in land cover mapping over large areas and considerable time scales (J. DONG and X. XIAO, 2016; T. N. PHAN et al, 2020; Y. PIAO et al, 2021; J. CUI et al, 2022; MIRMAZLOUMI et al, 2022). It is now a powerful tool for downloading and processing a wide variety of data simultaneously, in a consolidated system (N. SIDHU, 2018, ; N. A WAHAP and H. Z SHARFRI, 2020; T. N. PHAN et al, 2020). The different steps of this approach are presented in the following section.

## **MATERIALS & METHODS**

### **Presentation and characteristics of the study area**

The study area the DAA is located on the Ivorian coastline between 5°10'0" and 5°40'0" North Latitude and 4°30'0" and 4°60'0" West Longitude (figure 1). The shape of this sedimentary basin has been shaped by the Ebrié lagoon system that runs parallel to the coastline and separates the site into two morphological domains: the southern domain dominated by coastal

plains and the northern domain dominated by plateaus (BNEDT, 2008). The coastal plains have altitudes of less than 10 m, while those of the interior plateaus reach more than 200 m in places. This territory is dominated mainly by ferrallitic, hydromorphic, podzolic soils and by soils that are not very advanced on marine sands (E. ROOSE et al, 1966). These soils were originally covered by forest formations varying from the dense evergreen rainforest in the north and by swamp forests or mangroves in the south of the lagoon system (Y. T. BROU, 2018).

This vegetation cover has almost disappeared today due to the dynamics of the ADA. These dynamics, which began with the establishment of the Abidjan urban area as a capital in 1934, were reinforced with the opening of the Vridi canal and the development of the deep-water port in the early 1950s, and then exacerbated from 2002 onwards with the advent of the military-political crisis. This crisis, which lasted for about a decade, saw ADA receive a large number of people fleeing the Central, Northern and Western zones.

Figure 1: Location of the study area



ADA now has, in addition to the city subdivided into ten communes, four sub-prefectures, namely Anyama, Bingerville, Brofoudoumé and Songon. It covers approximately 2,034 km<sup>2</sup> with an estimated population of 6,321,017 inhabitants in 2021 (INS, 2021), i.e., a density of 3,108 hbt/km<sup>2</sup>. This significant anthropization is not without consequences for the vegetated areas.

### Study data

Tracking mapping of land cover index change was done through two reference dates 2002 and 2022 using Landsat 7 and 9 images from the Landsat Surface Reflectance Tier 1 orthorectified and atmospherically corrected image collections (Collection 2 Tier 1 calibrated top-of-atmosphere (TOA) reflectance, Table 1).

Table 1: Study Data

N°	Data	Path / Row	Resolution	Period (var start, var end)
1	LANDSAT_7 ETM +	196 / 56 et 195 / 56	30 m	01/01/2002 au 31/12/2002
2	LANDSAT_9 OLI-2 TIRS-2	196 / 56 et 195 / 56	30 m	01/10/2022 au 31/10/2022

Source: <https://earthengine.google.com>, <https://earthexplorer.usgs.gov/>

These are composite images created from the time periods var start Date and var end Date (table 1). The pre-processing and processing operations were done from these composite images. In fact, existing studies have shown that temporal aggregation methods and the use of one-, two-, and three-year mosaics lead to improved performance of classification results and better quality of land cover maps (A. J. OLIPHANT et al, 2019; D. N. RICHARDS and R. N. BELCHER, 2020; R. E. KENNEDY, 2021; Y. PIAO et al, 2021).

The choice of Landsat images is motivated by the fact that it is the only sensor to date whose images have covered the Earth's surface for more than 40 years at a spatial resolution of 30 m or 60 m for the first satellites and spectral bands that are generally consistent between the various sensors launched since 1972 (F. DUBERTRET et al., 2022, N. PHAN, 2020)

## **METHODS**

### **Choice of the classifier**

The mapping of land use indices through the GEE geospatial analysis platform is based on a number of algorithms such as Classification And Regression Trees (CART), K-Means, Gradient Boosting Regression (GBR), Machine Learning and Ensemble Algorithms (MLEA), The Support Vector Machine (SVM), The Minimum Distance (MD)... Remote sensing combining these algorithms reduces uncertainties related to land use changes in inaccessible areas (Y. PIAO et al, 2021). In this study, the approach is based on the supervised classification method using the Random Forest (RF) algorithm. Developed by Leo Breiman in 2001, RF or random forest is a combinatorial classification method based on categorical regression trees (L. BREIMAN, 2001; J. CUI et al, 2022).

This algorithm is applied to nonparametric statistical regression and classification problems based on a training dataset (K. TATSUMI et al, 2015; K. TATSUMI et al, 2016).

It consists of multiple independent and unrelated decision trees (Y. PIAO et al, 2021) and works by constructing multiple decision trees by outputting for each pixel the mode of all predicted classes (T. K. HO, 1998; F. DUBERTRET et al, 2022). The RF algorithm is currently perceived as one of the best and most widely used algorithms for classification with high accuracy of land cover from remote sensing data (M. PAL, 2005; X. LI et al, 2016; K. MILLARD and M. RICHARDSON, 2015; K. TATSUMI et al, 2016; N. P. THANH and M. KAPPAS, 2017; A. E. MAXWELL et al, 2018, M. AMANI et al, 2019, K. LOUKIKA et al, 2021). This method effectively solves the mixed pixel classification problem and achieves better classification results (I. X. FLOREANO and L. A DE MORAES, 2021; S. ZHANG et al, 2021).

### **Creation and pre-processing of a composite image**

The image pre-processing operations began with the import of the ADA polygon into the GEE platform, which allowed the working environment to be clipped and extracted. Time periods var start Date and var end Date (Table 1) were then set and applied to the Landsat Surface Reflectance Tier 1 products. The individual images are combined into a composite image using the median filter, which assigns each pixel an average over the period (K. LOUKIKA et al, 2021).

To the obtained mosaic was applied the function `map(maskL8srClouds)` in order to mask the permanent cloud covers that could bias the classification result. This function in GEE effectively solves the problems of cloud interference during the monsoon and the impossibility of using satellite image data during certain periods (Y. PIAO et al, 2021). This step is crucial in sub-equatorial regions such as the ADA where cloud cover is almost permanent all year round. These pre-processing operations allowed us to correct the images and improve their reflectance and visual quality.

### **Loading the training data and applying the classifier to the image**

For optimal accuracy of the classification results (R. GOLDBLATT et al, 2016, K. LOUKIKA et al, 2021), we added to the input Landsat image bands, four additional indices. These are the Normalized Difference Vegetation Index (NDVI), Normalized Difference Built-up Index (NDBI), Normalized Difference Modified Water Index (MNDWI), and the Modified Ground Adjusted Vegetation Index (MSAVI2). These indices calculated from two or more channels are designed to maximize vegetation, built-up, hydrography, and bare ground features respectively) while reducing noise (A. CICI, 2020; F. PECHMAY et al, 2022; N. PETTORELLI et al 2005; R. GOLDBLATT et al, 2016; Y. PIAO et al, 2021; Y. ZHA et al, 2003; H. XU, 2006; J. QI et al, 1994)

All of this data was added to the GEE environment from a Map.addLayer visualization dictionary. Training points were subsequently added and grouped into five dominant groups: Built, Forest, Gradient, Open, and Hydrography. The smile Random Forest classifier was finally built and applied to the composite image allowing this algorithm to discretize the spectral data into five land cover classes: "Built", "Forest", "Hydrography", "Orchard" and "Open".

### **Evaluation and improvement of classification results**

In order to test the robustness of the land use index discretization model, post-classification operations were necessary. The rasters obtained through the classification method of the RF algorithm were visually evaluated in order to detect possible classification errors or misclassified pixels based on the knowledge of our study area. Classification improvement was also done by comparing the land cover maps to archival Google Earth images (D. N. RICHARDS and R. N. BELCHER, 2020). Errors were corrected by adding additional training points in the parts

of the spectral space where confusion occurs. In addition, field missions were also performed. Following these classification and post classification operations, the robustness of the land cover mapping model in the DAA was assessed by the kappa coefficient and the overall accuracy index. This evaluation of the classifier accuracy was done by means of a confusion matrix (Confusion Matrix) (S. V. STEHMAN 1997; S. MAGNUSSEN, 2021).

### **Evaluation of changes in land use**

In order to statistically assess the different changes in the land use indices between 2002 and 2022, the results of the classification were exported to the ArcGis interface. The areas of the different classes were calculated from the attribute tables. Then, the different variations of the land cover classes were estimated using the Overall Rate of Change (equation 1), Average Annual Rate of Change (equation 2) and Absolute Difference (equation 3):

$$[1] \text{ ORC} = [(FY_2 - IY_1) / IY_1] \times 100$$

$$[2] \text{ AARC} = [(FY_2 / IY_1)^{1/t} - 1] \times 100$$

$$[3] \text{ AD} = FY_2 - IY_1$$

With  $IY_1$  = Initial Year area;  $FY_2$  = Final Year area and  $t$  = difference between the two years.

In addition to these quantities, spatial mutations were also determined from a transition matrix that discriminated the areal units of conservation, modification, and transformation.

## **RESULT**

The classification model using the RF algorithm was performed with an overall accuracy of 98.03% in 2002 and 98.7% in 2022 and kappa coefficients of 0.9 in 2002 and 2022. This model allowed to characterize the land use and to evaluate the mutations that occurred during this period.

### **Characterization of land use in the ADA in 2002 and 2022**

The land use in the DAA has been mapped according to five dominant land use indices.

The "Building" index, indicates old or ongoing settlements and housing areas. The "Forest" index groups together the relics of the tropical forest that originally predominated. The "Orchard" index refers to cocoa, rubber and oil palm plantations and other cash crops that have contributed to the decline in forest cover. The "Opened"

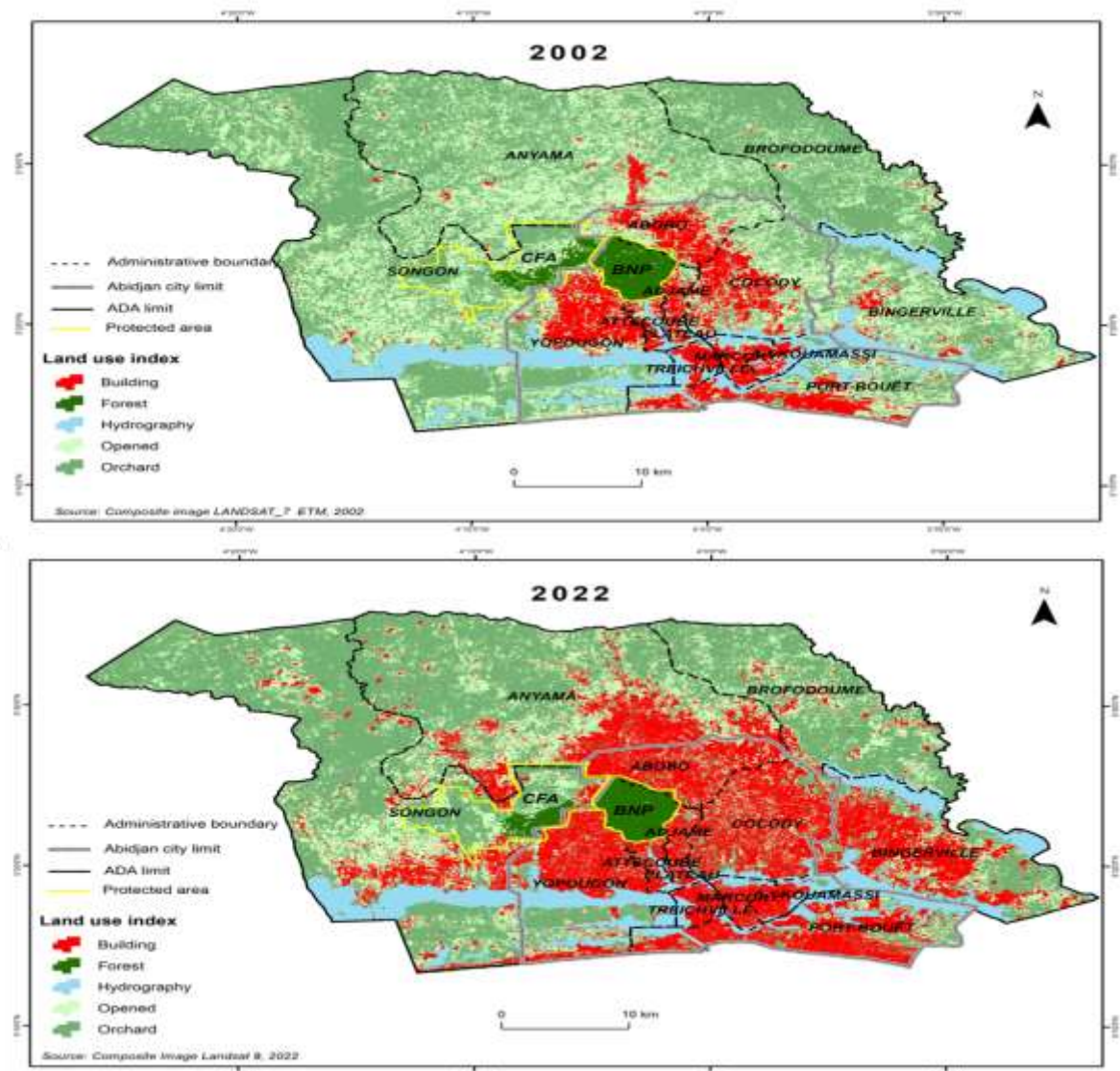
index refers to fields, fallows, open spaces or grass dominated areas. The "Hydrography" index refers to surface water present on a permanent or intermittent basis. Based on statistical (table 2) and the cartographic (figure 2) results, the ADA has been subject to significant land use and land cover changes over the past 20 years.

Table 2: Land use and land cover statistics in 2002 and 2022

Land use index	2002		2022		AD (km <sup>2</sup> )	ORC (%)	AARC (%)
	Aerae (km <sup>2</sup> )	(%)	Aera (km <sup>2</sup> )	(%)			
<b>Building</b>	204.7	10.1	554.8	27.3	350.1	171.01	5.11
<b>Orchard</b>	926.4	45.5	816.2	40.1	-110.2	-11.89	-0.63
<b>Opened</b>	658.8	32.4	434.6	21.4	-224.2	-34.03	-2.06
<b>Hydrography</b>	195.6	9.6	184.2	9.1	-11.4	-5.81	-0.30
<b>Forest</b>	48.4	2.4	44.1	2.2	-4.3	-8.94	-0.47
<b>Total</b>	2033.8	100	2033.8	100			

Source: Our treatments, 2023

Figure 2: Land use maps of the ADA in 2002 and 2022



In 2002, the use of land is reflected by a predominance (more than 45%) of individual or industrial plantations followed by open spaces (32.4%), residential areas and water surfaces (10%) and finally forest relics (2.4%) (table 2). During the last 20 years only the "Built" index has varied positively to pass from 20.4 thousand hectares in 2002 to more than 55.4 thousand hectares in 2022, that is to say a global increase of 171% and an average annual growth rate of 5.1% (table 2).

The "Opened" index has experienced the most important negative variation with more than 224 km<sup>2</sup> lost or 34% of its surface for

an annual decline rate of 2% (table 2). The plantations have also lost 110 km<sup>2</sup> or nearly 12% of their area (table 2). The forest relics that covered 48 km<sup>2</sup> in 2002 have declined by 9% equivalent to an area of 44 km<sup>2</sup>. The surfaces of water lost as for them more than 11 km<sup>2</sup> that is to say nearly 6% of their surface during these last 20 years.

### Changes in land use and land cover in the ADA between 2002 and 2022

The transition matrix (Table 3) provides a better understanding of these ongoing spatial changes over the past 20 years in the ADA.

Table 3: ADA Landscape Transition Matrix for 2002 to 2022

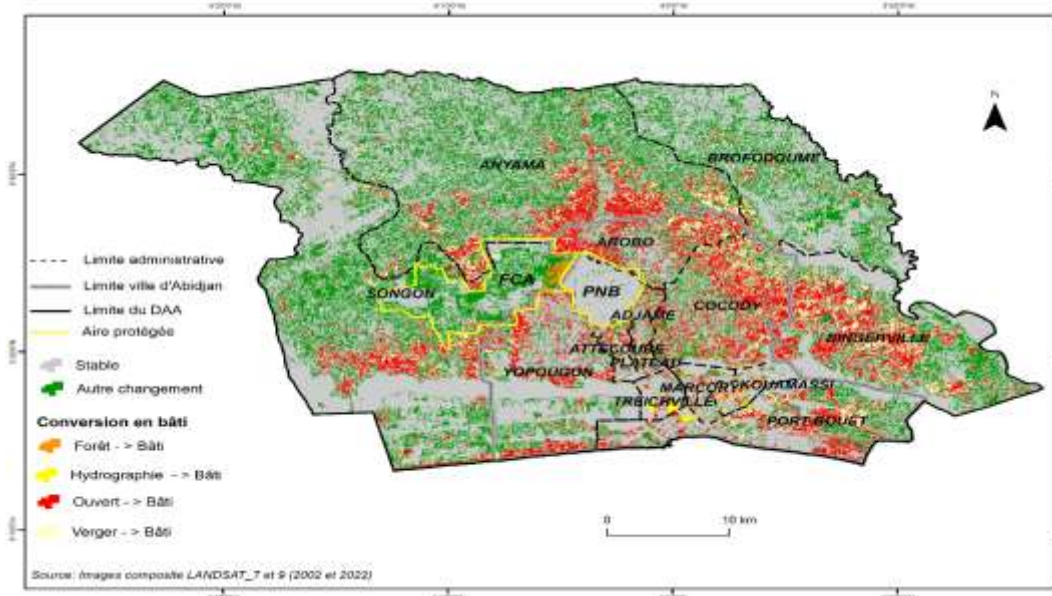
Land use index		2022 (km <sup>2</sup> )					TOTAL
		Building	Forest	Hydrography	Opened	Orchard	
2002 (km <sup>2</sup> )	Building	168,4	0,1	0,3	30,4	5,5	204,7
	Forest	2,9	39,2	0,03	2,6	3,6	48,4
	Hydrography	10,6	0,01	176,1	2,0	6,9	195,6
	Opened	234,6	3,8	5,3	186,3	228,6	658,8
	Orchard	138,2	1,0	2,5	213,2	571,3	926,4
	TOTAL	554,8	44,1	184,2	434,6	816,2	2033,8

Source: Our treatments, 2023

In total, during the period 2002 - 2022, 114 thousand hectares (56.1% of the total area) remained stable. The changes involved 45.8 thousand hectares and the conversions 43.3 thousand hectares or 22.6% and 21.6% of the total area of the District respectively.

Singularly, the conversion of land use indexes into built-up area concerned 38.6 thousand hectares or 89.1% of all conversions and 19% of all mutations that occurred during the period (Figure 3).

Figure 3: Changes between 2002 and 2022 in the ADA



This dynamic of housing to the detriment of other land uses is taking place in the direction of the new urban fronts of Cocody-Bingerville to the east, Abobo-Anyama-Brofodoumé to the north, and Yopougon-Songon to the west (figure 3). It is mainly at the expense of open spaces for 60.7% and plantations for 35.8%. Hydrographic surfaces such as the Ebrié

lagoon in particular are not exempt from this urbanization frenzy with approximately 3%. The waters of this body of water are drained mainly to the south of the ADA in the communes of Marcory, Treichville and Koumassi in order to gain land for building (figure 3). Photo 1 illustrates these development operations on the lagoon.

**Photo 1: Embankment operation on the lagoon in Koumassi**



The relics of the primary forest that are the Banco National Park (BNP) and the Classified Forest of Anguédédou (CFA), which are nevertheless located in protected areas, do not escape these anthropic pressures (figure 3) with a little less than 1%. These protected areas were created by decree of the colonial administration, the first in 1926 and the second in 1943, covering 4,200 and 8,447.47 hectares respectively. Illegal anthropic pressures (agricultural practices, urbanization and poultry farms) and legal pressures through successive declassification operations have caused the Anguédédou Classified Forest to lose nearly 90% of its surface area and the Banco National Park to lose about 18%.

## **DISCUSSION**

This study analyzes the changes in land use and land cover that have occurred in the ADA over the past two decades. The approach is based on the processing of Landsat composite images from 2002 and 2022 using the RF algorithm. As written by

S. ZHANG et al. (2021), the accuracy of classification results from remote sensing technology applied in the GEE platform environment depends on the chosen classification algorithm. The RF choice was motivated by feedbacks that conclude that this classifier is more robust compared to others (K. TATSUMI et al, 2016; M. BELGIU and L. DRĂGUȚ, 2016; D. ABIJITH and S. SARAVANAN, 2021; C. T. LIU et al, 2021; J. CUI et al, 2022). The results of this classification with an overall accuracy of more than 80% can be considered robust following the work of R. CONGALTON (1991), D. SYLLA et al (2021), J. CUI et al (2022), A. G. ADOU et al (2022), S. S. TRAORE et al (2022) and C. T. FAYE et al (2023).

Based on the results of this classification, the DAA is undergoing significant changes in land use and land cover. These changes particularly concern the vegetated areas that are inexorably being converted into urban areas. Thus, the space of two decades the habitat has experienced an increase of over



171% from 20.4 thousand hectares to 55.4 thousand hectares. This dynamic is accompanied mainly by a reduction in areas of crops and plantations that have lost 33.4 thousand hectares or 45.9% of their area in 2002.

This regressive dynamic of vegetation cover in favor of built-up areas is in agreement with the results of the work of F. A. MEMEL et al (2021), D. SYLLA (2021), J. CUI et al (2022), S. AMINI et al (2022) and PIAO et al (2021). This nibbling of agricultural land by the built-up area of cities is due to the existence of a land market that is unfavorable to the maintenance of agricultural activity (D. Sylla, 2021). The result is urban sprawl, which refers to the extent of urbanization due to population growth and large-scale migration that leads to changes in land use patterns (H. S. SUDHIRA et al, 2004).

In the ADA, as in many cities of the South, this often concentric urban sprawl guided by communication routes invades the surrounding countryside and progressively nibbles away at rural space (M. POULOT et al., 2012; J. CAVAILHES, 2004; D. SYLLA, 2021; K. I. N. RAHMI, 2022). Indeed, as in Kendari, Indonesia, urban expansion in the DAA is a centripetal process that starts from the center and spreads out to the surrounding areas (K. I. N. RAHMI, 2022). As cities stretch, they incorporate rural areas into the urban area similar to the finding of H. S. SUDHIRA et al. (2004) and R GOLDBLATT et al. (2016) in Indian urban areas. This urban sprawl is undeniably one of the potential threats (or the potential threat) to sustainable development, urban planning, efficient use of resources, and allocation of infrastructure initiatives in the urban South (H. S. SUDHIRA et al).

This change in land use and land cover caused by the development of urbanization and industrialization undoubtedly leads to the degradation of vegetation cover and sustainable conditions for the future (D. ABIJITH and S. SARAVANAN, 2021). This observation is corroborated by the

results of S. S. TRAORE (2022) around the mining sites in southern Mali. This degradation of vegetation due to sustained population growth does not spare protected areas. As noted by R. K. OURA (2012), SAKO N et al (2013) N. SAKO and G. BELTRANDO (2014), Y. M. A. D.-C. OBOUE and K. E. KONAN (2022) the Banco National Park and the Anguédédou Classified Forest, which are essential to the ecosystemic balance, are subject to daily pressures due to the activities and rapid urbanization of the ADA.

In the face of these challenges, accurate, current, and long-term information on land use and land cover remains essential not only for local development but also for government policies (T. N. PHAN, 2020). Quantifying and monitoring the spatial and temporal dynamics of land use then appear essential to better understand many land surface processes (A. MIDEKISA et al, 2017). Well conducted, this monitoring undeniably constitutes decision-making and territorial planning support tools for the preventive management of extreme social and environmental crises.

## **CONCLUSION**

The ADA is experiencing a continuous loss of vegetated areas, particularly in favor of urban areas. This expansion of habitat, in conjunction with exceptional demographic growth and the polarization of economic activity by the ADA, contributes to the loss of vitality of natural ecosystems, the degradation of protected areas and the retreat of agricultural spaces.

The classification approach using the Random Forest algorithm in the Google Earth Engine platform certainly has inherent limitations, particularly due to the relatively high quality and spatial resolution (30 m) of the input Landsat satellite images. Images with spatial resolution at the centimetre level using sensors such as drones would allow for better refinement of the results of this classification.

In fact, monitoring and mapping of land use and land cover are undeniably tools for

decision support, territorial planning and sustainable development. Future studies should also focus on modeling and predicting the dynamics of land use in this capital city in the territorial framework of Côte d'Ivoire.

### Declaration by Authors

**Acknowledgement:** We would like to express our gratitude to the Programme d'Appui Stratégique à la Recherche Scientifique en Côte d'Ivoire (PASRES), the Fonds National pour la Science, la Technologie et l'Innovation (FONSTI) and the Centre Suisse de Recherche Scientifique (CSRS) for agreeing to finance the research of which a part of the results is presented in this article.

**Source of Funding:** None

**Conflict of Interest:** The authors declare no conflict of interest.

### REFERENCES

1. ABIJITH D. et SARAVANAN S. (2021). Assessment of land use and land cover change detection and prediction using remote sensing and CA Markov in the northern coastal districts of Tamil Nadu, India, *Environmental Science and Pollution Research*, [En ligne], p. 1-13.
2. ADOU A. G., KOUAO N. S. R., YAO-KOUASSI Q. C. et ALLA DELLA A., (2022). Dynamique d'expansion des vergers d'anacardiés et transformation du paysage en zone forestière dans un contexte de transition écologique : cas des finages de la sous-préfecture de Vavoua (centre-ouest de la Côte d'Ivoire), *Revue de géographie du laboratoire Leïdi*, n°27, p. 1-23
3. AMANI M., MAHDAVI S.; AFSHAR M.; et al., (2019). Canadian Wetland Inventory using Google Earth Engine: The First Map and Preliminary Results, *Remote Sens.*, [En ligne], vol. 11, n°7.
4. AMINI S., SABER M., RABIEI-DASTJERDI H., and HOMAYOUNI S. (2022). Urban Land Use and Land Cover Change Analysis Using Random Forest Classification of Landsat Time Series. *Remote Sens.* [En ligne], Vol. 14, p. 1- 23.
5. BELGIU M. et DRĂGUȚ L. (2013). Random forest in remote sensing, A review of applications and future directions. *ISPRS J. Photogramm. Remote Sens.*, [En ligne], vol. 114, p. 24–31.
6. BENINDE J.; VEITH M.; HOCHKIRCH A. (2015). Biodiversity in cities needs space: A meta-analysis of factors determining intra-urban biodiversity variation. *Ecol. Lett.*, 18, 581–592.
7. BREIMAN L. (2001). Random forests, *Machine learning*, vol. 45, n° 1, p. 5-32.
8. BROU Y. T. (2008). La végétation du littoral ivoirien, *Géographie du littoral de Côte d'Ivoire : éléments de réflexion pour une politique de gestion intégrée*, La clonerie Saint-Nazaire, pp 23-36.
9. CASU F.; MANUNTA M.; AGRAM P.S.; CRIPPEN R.E. (2017). Big Remotely Sensed Data: Tools, Applications and Experiences, *Remote Sens. Environ.*, [En ligne], vol. 202, p. 1–2.
10. CAVAILHES J. (2004). L'extension des villes et la périurbanisation, In *Villes et économie*. Éd., Institut des villes, La Documentation Française, 157-184.
11. CICI A. (2020). Normalised difference spectral indices and urban land cover as indicators of land surface temperature (LST). *Int. J. Appl. Earth Obs. Geoinf.*, [En ligne], vol. 86, p. 1-11.
12. CONGALTON R., (1991). A review of assessing the accuracy of classifications of remotely sensed data. *Remote sensing of environment*, [En ligne], vol. 37, n° 1, p. 35-46.
13. CUI J., ZHU M., LIANG Y. et al., (2022). Land use/land cover change and their driving factors in the Yellow River Basin of Shandong Province based on google earth Engine from 2000 to 2020., *ISPRS International Journal of Geo-Information*, [En ligne], vol. 11, n°163, p. 1-18
14. DALLIMER M.; TANG Z.; BIBBY P.R.; and al, (2011). Temporal changes in greenspace in a highly urbanized region. *Biol. Lett.* 2011, [En ligne], vol. 7, p. 763–766.
15. DONG J. and XIAO X. (2016). Evolution of regional to global paddy rice mapping methods: A review. *ISPRS J. Photogramm. Remote Sens.*, [En ligne], vol. 119, p. 214–227.
16. DUBERTRET F., LE TOURNEAU F.-M., VILLARREAL M. L., et al. (2022). Monitoring Annual Land Use/Land Cover Change in the Tucson Metropolitan Area with Google Earth Engine (1986–2020), [En

- ligne], *Remote Sensing*, vol. 14, no 9, p. 21-27.
17. ELMQVIST T.; SETÄLÄ H.; HANDEL S.N.; VAN DER PLOEG S.; ARONSON J.; BLIGNAUT J.N.; GÓMEZ-BAGGETHU, E.; NOWAK D.J.; KRONENBERG J.; DE GROOT R. (2015). Benefits of restoring ecosystem services in urban areas. *Curr. Opin. Environ. Sustain.*, 14, 101–108.
  18. FAYE C. T., THIAW A. D. et FAYE G.. (2023). Dynamique du couvert végétal dans la Forêt Communautaire de Sambandé au Sénégal », *Physio-Géo* [En ligne], Volume 19 | 2023, mis en ligne le 20 mars 2023, consulté le 03 avril 2023.
  19. FLOREANO I. X., and DE MORAES L. A. F. (2021). Land use/land cover (LULC) analysis (2009–2019) with Google Earth Engine and 2030 prediction using Markov-CA in the Rondônia State, Brazil. *Environmental Monitoring and Assessment*, [En ligne], vol. 193, no 4, p. 1-17.
  20. GOLDBLATT R., YOU W., HANSON G., and KHANDELWAL A. K. (2016). Detecting the boundaries of urban areas in india: A dataset for pixel-based image classification in google earth engine. *Remote Sensing*, vol. 8, n° 8, p. 634.
  21. GORELICK N.; HANCHER M.; DIXON M.; ILYUSHCHENKO S.; THAU D.; MOORE R. (2017). Google Earth Engine: Planetary-Scale Geospatial Analysis for Everyone. *Remote Sens. Environ.*, vol. 202, p. 18–27.
  22. GROUPE DE LA BANQUE MONDIALE (2019). Que la route soit belle : Améliorer la mobilité urbaine à Abidjan, Huitième rapport sur la situation économique en Côte d’Ivoire, [en ligne], 64 P.
  23. HO T.K. (1998). The Random Subspace Method for Constructing Decision Forests, [En ligne], *IEEE Trans. Pattern Anal. Mach. Intell.*, Vol. 20, p. 832–844.
  24. INSTITUT NATIONAL DE LA STATISTIQUE (INS) (1992). Répartition spatiale de la population et migrations, Tome 2, Analyse des résultats définitifs du RGPH-88, Abidjan
  25. INSTITUT NATIONAL DE LA STATISTIQUE (INS) (2001). Recensement Général de la Population et de l’Habitat 98 : Migration – urbanisation, Volume 4, Tome 2, Abidjan, INS
  26. INSTITUT NATIONAL DE LA STATISTIQUE (INS-SODE) (2014). *Recensement Général de la Population et de l’Habitat (RGPH) 2014, Répertoire des localités : District Autonome d’Abidjan*, Abidjan, 13 p.
  27. KENNEDY R. E. (2021). Land Cover and Land Use Classification» in Google Earth Engine. © World Bank. [En ligne], License: Creative Commons Attribution license (CC BY 3.0 IGO),
  28. KOSCHKE L.; FÜRST C.; FRANK S. and MAKESCHIN F., (2012). A multi-criteria approach for an integrated land-cover-based assessment of ecosystem services provision to support landscape planning, *Ecol. Indic.*, [En ligne], vol 21, p. 54–66,
  29. LAI H.; FLIES E.J.; WEINSTEIN P.; WOODWARD A. (2019). The impact of green space and biodiversity on health, *Frontiers in Ecology and the Environment*, 2019, vol. 17, no 7, p. 383-390.
  30. LI X.; CHEN W.; CHENG X.; WANG L. (2016). A Comparison of Machine Learning Algorithms for Mapping of Complex Surface-Mined and Agricultural Landscapes Using ZiYuan-3 Stereo, Satellite Imagery. *Remote Sens.*, [En ligne], vol. 8, n° 6, p. 1-27.
  31. LIU C.T.; FENG Q.L.; JIN D.J.; and al., (2021). Application of random forest and Sentinel-1/2 in the information extraction of impervious layers in Dongying City, *Remote Sens. Nat. Resour.*, [En ligne], vol. 33, n°3 p. 253–261.
  32. LOUKIKA K., REDDY N. V. K. and SRIDHAR V. (2021). Analysis of land use and land cover using machine learning algorithms on Google Earth Engine for Munneru River Basin, India. *Sustainability*, [En ligne], vol. 13, p. 1- 15.
  33. MAXWELL A. E.; WARNER T. A.; FANG F. (2018). Implementation of machine-learning classification in remote sensing:an applied review, *Inter. J. Remote Sens.*, [En ligne], vol. 39, n° p. 2784–2817.
  34. MEMEL F. A. et AKADJÉ M-C. L. (2021). Impact spatial d’un équipement urbain : le cas de l’autoroute Abidjan- Accra, à Grand-Bassam, Colloque international « Gouvernance, économie et Société : l’Afrique face aux défis du XXI ème siècle », 20 au 22 Mai 2021 à l’Université Jean Lorougon Guédé de Daloa, Volume 2, Nouvelles Editions Balafons (NEB), 2021, pp. 641-673.

35. MIDEKISA A., HOLL F., SAVORY D. J., and al, (2017). Mapping land cover change over continental Africa using Landsat and Google Earth Engine cloud computing. *PloS one*, [En ligne], vol. 12, no 9, p. 1-15.
36. MAGNUSSEN S. (2021). Calibration of a Confidence Interval for a Classification Accuracy, *Open Journal of Forestry*, vol. 11, no 1, p. 14-36.
37. MILLARD K.; and RICHARDSON M. (2015). On the Importance of Training Data Sample Selection in Random Forest Image Classification: A Case Study in Peatland Ecosystem Mapping, *Remote Sens.*, [En ligne], vol. 7, no 7, p. 8489-8515.
38. MIRMAZLOUMI S.M.; KAKOOEI M.; MOHSENI F.; and al (2022). ELULC-10, a 10 m European Land Use and Land Cover Map Using Sentinel and Landsat Data in Google Earth Engine, *Remote Sens*, [En ligne], vol. 14, 3041.<https://doi.org/10.3390/rs14133041>
39. NIQUISSE S.; CABRAL P.; RODRIGUES Â.; AUGUSTO G., 2017. Ecosystem services and biodiversity trends in Mozambique as a consequence of land cover change, *Inter. J. Biodivers. Sci. Ecosyst. Serv. Manag*, [En ligne], vol. 13, no 1, p. 297-311.
40. OBOUE Y. M. A. D.-C. et KONAN K. E. (2022). Evolution spatio-temporelle de la Forêt classée d'Anguededou, une des dernières reliques forestières de la ville d'Abidjan dans le Sud-ouest de la Côte d'Ivoire, *Regardssud*, N° 1-2022
41. OLIPHANT A. J., THENKABAIL P. S., TELUGUNTLA P., et al. (2019). Mapping cropland extent of Southeast and Northeast Asia using multi-year time-series Landsat 30-m data using a random forest classifier on the Google Earth Engine Cloud. *International Journal of Applied Earth Observation and Geoinformation*, vol. 81, p. 110-124.
42. OSSENI A. A., GBESSO G. H. F., IDAKOU G. N., FANDOHAN A. B., TOKO I., TENTE A. B. H. et SINSIN B. A (2023). Reconstitution spatiale et simulation des changements futurs de l'occupation du sol dans la Réserve de Biosphère de la basse vallée de l'Ouémé (RB-BVO) au Bénin, *Physio-Géo* [En ligne], Volume 19 | 2023, mis en ligne le 02 février 2023, consulté le 03 avril 2023.
43. OURA R. K., (2012). Extension urbaine et protection naturelle : La difficile expérience d'Abidjan , *VertigO - la revue électronique en sciences de l'environnement* [En ligne], Volume 12 Numéro 2 | septembre 2012, mis en ligne le 31 octobre 2012, consulté le 03 novembre 2022.
44. PAL M. (2005). Random Forest Classifier for Remote Sensing Classification, *Int. J. Remote Sens.*, vol. 26, [En ligne], vol. 26, no 1, p. 217-222.
45. PECH-MAY F., AQUINO-SANTOS R., RIOS-TOLEDO G. et al., (2022). Mapping of land cover with optical images, supervised algorithms, and google earth engine, *Sensors*, [En ligne], vol. 22, n° 13, p. 1-19.
46. PETTORELLI N.; VIK J.O.; MYSTERUD A.; and al. (2005). Using the satellite-derived NDVI to assess ecological responses to environmental change, *Trends Ecol. Evol.*, [En ligne], vol. 20, p. 503–510.
47. PHAN T. N., KUCH V. and LEHNERT L. W. (2020). Land Cover Classification using Google Earth Engine and Random Forest Classifier—The Role of Image Composition, *Remote Sensing*, [En ligne], vol. 12, no 15, p. 2411.
48. PHAN T. N., KUCH V. et LEHNERT L. W. (2020). Land cover classification using Google Earth Engine and random forest classifier—The role of image composition. *Remote Sensing*, vol. 12, no 15, p. 2411.
49. PIAO Y., JEONG S., PARK, S., et al. (2021). Analysis of land use and land cover change using time-series data and random forest in North Korea. *Remote Sensing*, [En ligne], vol. 13, no 17, 3501.<https://doi.org/10.3390/rs13173501h>
50. POULOT M., ARAGAU C. and LAVUE, M. (2012). Habiter en périurbain ou réinventer la qualité de la ville. *Historiens & Géographes*, [En ligne], 419, 119-126
51. QI J., CHEHBOUNI A., HUETE A. R., et al., (1994). A modified soil adjusted vegetation index. *Remote sensing of environment*, [En ligne], vol. 48, no 2, p. 119-126.
52. RAHMI K. I. N., ALI A., MAGHRIBI A. A., and al., (2022). Monitoring of land use land cover change using google earth engine in urban area: Kendari city 2000-2021. In : IOP Conference Series: *Earth and Environmental Science*. IOP Publishing,.

- [En ligne], p. 1-9. doi:10.1088/1755-1315/950/1/012081
53. RICHARDS D. R.; and BELCHER R.N., (2020). Global changes in urban vegetation cover, *Remote Sens.*, [En ligne], vol. 12, 23.
54. ROOSE E., CHÉROUX M., HUMBEL F., et al. (1966). Les sols du bassin sédimentaire de Côte d'Ivoire, *Cahiers ORSTOM*, série pédologie, vol. 4, p. 51-92.
55. ROY D. P.; WULDER, M. A.; LOVELAND T. R. and al., (2014). Landsat-8: Science and product vision for terrestrial global change research., *Remote Sens. Environ.*, [En ligne], vol 145, p. 154–172, doi:10.1016/j.rse.2014.02.001.
56. SAKO N., BELTRANDO G., ATTA K. L., N'DA H. D. et BROU T.. (2013). Dynamique forestière et pression urbaine dans le Parc national du Banco (Abidjan, Côte d'Ivoire), *VertigO-la revue électronique en sciences de l'environnement*, vol. 13, no 2.
57. SAKO N. et BELTRANDO G. (2014). Dynamiques spatiales récentes du Parc National du Banco (PNB) et stratégies de gestion communautaire durable de ses ressources forestières (District d'Abidjan en Côte d'Ivoire)", *EchoGéo* [Online], 30 | 2014, Online since 17 September 2014, connection on 01 August 2021.
58. SIDHU N., PEBESMA E. and CÂMARA G., (2018). Using Google Earth Engine to detect land cover change: Singapore as a use case, *European Journal of Remote Sensing*, [En ligne], vol. 51; n°1, p. 486-500, Doi: 10.1080/22797254.2018.1451782
59. STEHMAN S. V. (1997). Estimating standard errors of accuracy assessment statistics under cluster sampling. *Remote Sensing of Environment*, [En ligne], vol. 60, no 3, p. 258-269.
60. SUDHIRA H. S., RAMACHANDRA T. V., and JAGADISH K. S. (2004). Urban sprawl: metrics, dynamics and modelling using GIS., *International Journal of Applied Earth Observation and Geoinformation* , [En ligne], vol. 5, no 1, p. 29-39.
61. SYLLA D. et AKADJE-KONAN L. M-C, (2022). La zone humide de Grand-Bassam face aux enjeux fonciers et aux besoins d'extension de la métropole abidjanaise, *DaloGéo*, Revue de Géographie de l'Université de Daloa, Deuxième numéro spécial, p. 11-22
62. SYLLA D. (2021). Cartographie des acquisitions foncières à la périphérie de la métropole abidjanaise, *Bulletin de la Société Géographique de Liège* [En ligne], vol. 77, n° (2021/2)- Varia, 33-43
63. SYLLA D., KOUASSI A., HAUHOUCOT C., (2021). Évolution de la forêt classée de N'Ganda N'Ganda (Assinie, Côte d'Ivoire) d'après la comparaison de deux images Landsat de 1987 et 2018. *Photo Interpretation European Journal Of Applied Remote Sensing*, [En ligne], vol. 56-57, p. 21-27.
64. TATSUMI K., YAMASHIKI Y., MORANTE A. K. M., et al. (2016). Pixel-based crop classification in Peru from Landsat 7 ETM+ images using a Random Forest model., *Journal of Agricultural Meteorology*, [En ligne], vol. 72, no 1, p. 1-11.
65. TATSUMI K., YAMASHIKI Y., TORRES M. A. C., AND TAIPE C. L. R. et al., (2015). Crop classification of upland fields using Random forest of time-series Landsat 7 ETM+ data., *Computers and Electronics in Agriculture*, [En ligne], vol. 115, p. 171-179.
66. THANH N. P. and KAPPAS, M., 2017. Comparison of Random Forest, k-Nearest Neighbor, and Support Vector Machine Classifiers for Land Cover Classification Using Sentinel-2 Imagery. *Sensors*, [En ligne], vol. 18, 18.
67. TRAORE S. S., DEMBELE S., DEMBELE D., DIAKITE N. et DIAKITE C. H. (2022). Dynamique de l'occupation du sol et trajectoire du couvert végétal autour de trois sites miniers du Sud Mali entre 1988 et 2019, *Physio-Géo* [En ligne], Volume 17 | 2022, mis en ligne le 18 septembre 2022, consulté le 03 avril 2023.
68. TZOULAS K.; KORPELA K.; VENN S.; YLI-PELKONEN V.; KA'ZMIERCZAK A.; NIEMELA J.; JAMES P. (2007). Promoting ecosystem and human health in urban areas using Green Infrastructure: A literature review. *Landsc. Urban Plan.*, 81, 167–178.
69. UNITED NATIONS, Department of Economic and Social Affairs, Population Division, (2019). World Urbanization Prospects: The 2018 Revision. Online Edition, <https://population.un.org/wup/Download/>

70. WAHAP N. A. and HELMI H. Z. (2020). Utilization of Google earth engine (GEE) for land cover monitoring over Klang Valley, Malaysia; *IOP Conference Series: Earth and Environmental Science*, [En ligne], vol. 540. No. 1. IOP Publishing.
71. WULDER M.A.; COOPS N.C.; ROY D.P.; WHITE J.C.; HERMOSILLA T. (2018). Land Cover 2.0. *Int. J. Remote Sens.*, Vol. 39, p. 4254–4284.
72. WULDER M.A.; WHITE J.C.; LOVELAND, T. R.; et al, (2016). The global Landsat archive: Status, consolidation and direction, *Remote Sens. Environ.*, [En ligne], vol. 185, p. 271–283, doi:10.1016/j.rse.2015.11.032.
73. XIE S.; LIU L.; ZHANG X.; YANG J.; CHEN X.; GAO Y. (2019). Automatic Land-Cover Mapping Using Landsat Time-Series Data Based on Google Earth Engine. *Remote Sens.*, [En ligne], 11, 3023.
74. XU J.; XIAO W.; HE T.; DENG X.; CHEN W. (2021). Extraction of Built-up Area Using Multi-Sensor Data—A Case Study Based on Google Earth Engine in Zhejiang Province, China. *Int. J. Remote Sens.*, [En ligne], 42, 389–404.
75. XU, H.. (2006). Modification of normalised difference water index (NDWI) to enhance open water features in remotely sensed imagery, *International journal of remote sensing*, [En ligne], vol. 27, no 14, p. 3025-3033.
76. ZHA Y., GAO J., & NI,S., (2003). Use of Normalized Difference Built-Up Index in Automatically Mapping Urban Areas from TM Imagery, *International Journal of Remote Sensing*, [En ligne], vol.24, no. 3: p. 583-594.
77. ZHA Y.; GAO J.; Ni S., (2003). Use of normalized difference built-up index in automatically mapping urban areas from TM imagery, *Int. J. Remote Sens.*, [En ligne], vol. 24, p. 583–594.
78. ZHANG S., YANG P., XIA J., et al. (2021). Land use/land cover prediction and analysis of the middle reaches of the Yangtze River under different scenarios, *Science of the Total Environment*, [En ligne], 46 p

How to cite this article: Kinakpefan Michel Traore. Monitoring of land use dynamics in the autonomous district of abidjan between 2002 and 2022 using the google earth engine platform. *International Journal of Research and Review*. 2023; 10(5): 255-268. DOI: <https://doi.org/10.52403/ijrr.20230532>

\*\*\*\*\*